

# An Inexpensive, Widely Available Material for 4 wt % Reversible Hydrogen Storage Near Room Temperature

Tod A. Pascal,<sup>†,‡</sup> Christopher Boxe,<sup>§</sup> and William A. Goddard, III<sup>\*,†,‡</sup>

<sup>†</sup>Material and Process Simulation Center, California Institute of Technology, Pasadena, California 911205, United States

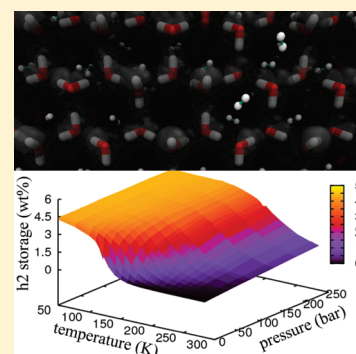
<sup>‡</sup>Graduate School of EEWS (WCU), Korea Advanced Institute of Science and Technology, Daejeon, Korea

<sup>§</sup>Earth and Planetary Science Division, NASA Jet Propulsion Laboratories, Pasadena, California 91109, United States

**S** Supporting Information

**ABSTRACT:** The search for cheap, renewable energy sources to replace fossil fuels has identified hydrogen gas (H<sub>2</sub>) as the most promising, particularly for transportation. However, despite intense research efforts to find reliable storage materials, current practical technologies store only 1.3 wt % H<sub>2</sub> at 270 K, far short of the U.S. DOE targets. We report that hexagonal ice, the ordinary form of ice in snow, may be an efficient hydrogen storage material, achieving 3.8 wt % H<sub>2</sub> storage and 42 g L<sup>-1</sup> at 150 K and that after loading at 150 K, the 3.8 wt % H<sub>2</sub> can be kept at 270 K and then released upon heating by a few degrees Kelvin. This leads us to propose the ice-fixed melt-triggered (IFMT) strategy for hydrogen storage and utilization with ice as the median.

**SECTION:** Energy Conversion and Storage



Hydrogen has been identified as a most promising fuel for meeting our future energy needs; however, there are difficulties in storage and retrieving the hydrogen once stored.<sup>2</sup> Metal-based and chemical storage systems are capable of storing sufficient H<sub>2</sub> to meet the US DOE goals for transportation,<sup>3</sup> however, they involve H–H bond breaking and formation processes that lead to rates that are far too slow for modern applications. Systems based on physisorption of the H<sub>2</sub> molecules have sufficient rates, but the adsorption energies are low, so that the best-performing such material, MOF-177, stores only 1.3% wt H<sub>2</sub> at 270 K.<sup>4</sup>

Hexagonal ice (ice Ih) is the natural form of ice in snow and the upper atmosphere, and is the thermodynamically favored ice phase from 180 to 273 K and 0 to 1 GPa (10 000 bar  $\approx$  10 000 atm). It has an unusually low packing fraction (0.43) and density (0.92 g/mL). The internal pore diameter is small ( $\approx$  0.23 nm) but we find that it can accommodate dihydrogen (H<sub>2</sub>) molecule. Indeed using quasielastic neutron scattering experiments, Strauss et al.<sup>5</sup> showed that H<sub>2</sub> has a remarkably high diffusion constant in hexagonal D<sub>2</sub>O at low temperatures (60 K),  $D = 9.5 \times 10^{-5}$  cm<sup>2</sup>/s, comparable to the diffusion constant of H<sub>2</sub> in liquid hydrogen ( $D = 14 \times 10^{-5}$  cm<sup>2</sup>/s at 25 K). Some reports indicate that little dihydrogen dissolves in ice near freezing at low pressures (100 bar),<sup>6,7</sup> but it is known that H<sub>2</sub> is 25% more soluble in ice than water.<sup>8</sup>

There is some evidence that hydrogen can form stable solutions with ice-like motifs at ambient pressures.<sup>9</sup> Thus Mao and Mao<sup>10</sup> found 5.3 wt % storage in hydrogen clathrate hydrate at 77 K and 2 kbar while Lee and co-workers<sup>11</sup> reported  $\sim$ 4 wt % hydrogen storage in THF-containing binary-clathrate hydrates at

freezing temperature and around 120 bar. Additionally, Dyadin and co-workers<sup>12</sup> showed that significant amounts of H<sub>2</sub> and at least 10 wt % He dissolve in ice Ih (D<sub>2</sub>O) at 2–3 kbar, increasing the melting temperature by at least 10 K relative to perfect ice crystals. Also Londono and co-workers<sup>13</sup> showed experimentally that helium dissolves in ice II at 2.8 kbar to form stable He<sub>x</sub>-(D<sub>2</sub>O)<sub>6</sub> structures.

In this letter, we report the hydrogen storage capability of ice Ih using first-principles-based computer simulations (with interaction potentials based on accurate quantum mechanics). In order to accurately describe the interactions of H<sub>2</sub> with H<sub>2</sub>O for large scale molecular dynamics (MD) and Monte Carlo (MC) simulations, we developed a classical force field (FF) fitted to potential energy surfaces of H<sub>2</sub>–H<sub>2</sub>O<sup>14</sup> and the H<sub>2</sub> dimer<sup>15</sup> derived from accurate quantum mechanics (QM) calculations, in conjunction with the empirical TIP4P/ice water potential<sup>1</sup> (Table 1 and Figure S1 (Supporting Information)). This approximation of rigid H<sub>2</sub> and rigid porous framework is validated by the good agreement with experiment for H<sub>2</sub>/MOF and H<sub>2</sub>/COF systems (see ref 21) and by the good agreement with

- the experimental H<sub>2</sub> dimer equation of state (EOS)<sup>16</sup> from 100–270 K and 0–250 bar (Figure S2),
- the self-diffusion constant of H<sub>2</sub> in ice Ih at 60 K<sup>5</sup> (Figure S3), and
- the shift in melting temperature of hydrogen loaded ice Ih under pressure<sup>12</sup> (Table S2),

**Received:** April 4, 2011

**Accepted:** May 24, 2011

**Published:** May 24, 2011

**Table 1. Short-Range van der Waals (vdW) and Hydrogen-Bonding (HB) Interaction Parameters for H<sub>2</sub>–H<sub>2</sub>O Used in This Study<sup>a</sup>**

Interaction pair	Type <sup>b</sup>		vdW			Dreiding H-bond <sup>d</sup>		p
			De (kcal/mol)	Re (Å)	ξ	De (kcal/mol)	Re (Å)	
Ow	Ow	LJ12–6	0.2110	3.5546	n/a	n/a		
Ow	H <sub>-</sub>	Exp-6	0.1349	3.1932	11.44	n/a		
Hw	H <sub>-</sub>	Exp-6	0.0011	3.4061	14.88	n/a		
H <sub>-</sub>	H <sub>-</sub>	Exp-6	0.0209	3.1596	11.44	n/a		
Hm <sup>c</sup>	Ow <sup>d</sup>	n/a				0.0174	3.5827	1

<sup>a</sup>  $E_{hbond} = D_e \{ 5\rho^{-12} - 6\rho^{-10} \} \cos^p(\theta)$ ,  $\rho = (R_c)/(R)$  <sup>b</sup>  $E_{vdw}^{LJ12-6} = D_e \{ \rho^{-12} - 2\rho^{-6} \}$ ,  $E_{vdw}^{Exp-6} = (D_e)/((\xi - 6)) \{ 6e^{\xi(1-\rho)} - \xi\rho^{-6} \}$  <sup>c</sup> donor <sup>d</sup> acceptor  
<sup>a</sup> The H<sub>2</sub>–H<sub>2</sub>O and H<sub>2</sub>–H<sub>2</sub> interactions are obtained from fitting the ab initio potential energy surfaces obtained at the CC or MP2 level needed to accurately predict London dispersion (vdW attraction). The water molecules are modeled using the rigid TIP4P-ice<sup>1</sup> FF. The atom types are: Ow (oxygen on water), Hw (hydrogen on water), H<sub>-</sub> (hydrogen on H<sub>2</sub>), Hm (pseudo-atom at the H<sub>2</sub> bond midpoint). Interactions not shown are zero. Our model includes Coulombic interactions based on the following fixed point charges (in electron units): Ow (–1.1794 displaced from atom center by 0.1577 Å), Hw (+0.5897), H<sub>-</sub> (+0.36535) and Hm (–0.7307).

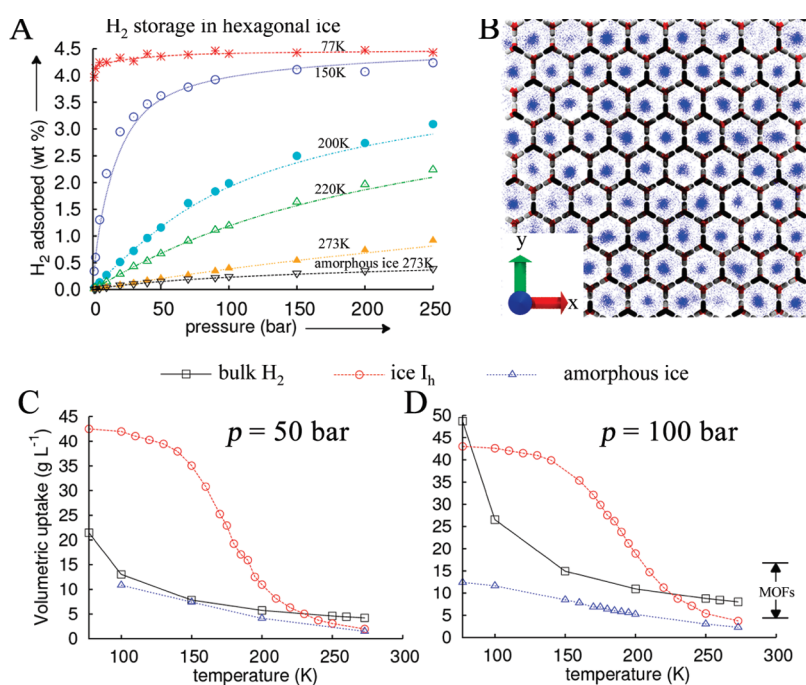


**Figure 1.** (A) Average loading of H<sub>2</sub> molecules in ice Ih predicted from GCMC simulations from 1 to 250 bar at 77 K (red stars), 150 K (blue circles), 200 K (cyan filled circles), 220 K (green upward triangles), 273 K (orange upward triangles) compared to amorphous ice at 273 K (black downward triangles). (B) Two dimensional plot of the H<sub>2</sub> density profile in the ice Ih channels at 150 K and 100 bar projected along the z axis. The H<sub>2</sub> molecules are at the center of the hexagonal channel with ~1 molecule per fundamental unit cell (12 water molecules). (C) Volumetric loading curve at 40 bar for H<sub>2</sub> in ice Ih (red circles), amorphous ice (blue triangles) compared to an open tank (black squares). (D) Volumetric 100 bar loading curve for H<sub>2</sub>. The range of values for MOFs at 300 K is shown as a reference.

suggesting that our FF and simulation methodology is accurate.

Using this QM derived FF, we used grand canonical Monte Carlo (GCMC) simulations<sup>17,18</sup> to predict the loading of H<sub>2</sub> in ice Ih crystal.<sup>19,20</sup> We showed previously that this GCMC methodology successfully predicts the hydrogen uptake in metal organic frameworks (MOFs) in excellent agreement with experiment.<sup>21</sup>

Figure 1a shows the gravimetric hydrogen uptake percent of ice Ih from 77 to 273 K and 1 to 250 bar. We find 3.96 wt % at 77 K and 1 bar, which is 75% larger than MOF-200 (using similar calculations) and twice that measured and calculated for MOF-177. Among the plethora of ice structures available

in nature, ice Ih seems to be best suited for hydrogen storage since it has the lowest density and largest pore size. Indeed the GCMC density profiles (Figure 1b and Figures S4 and S5) show that most H<sub>2</sub> molecules occupy interstitial sites, preferentially located in the center of the hexagonal channels. In contrast, we find that amorphous ice stores only 1/4 as much H<sub>2</sub> at 77 K and 1 bar. The 77 K isotherm for ice Ih saturates to 4.4 wt % at 40 bar, which can be compared to 7.5 wt % and 70 bar for MOF-177 and 8.7 wt % and 60 bar for MOF-200. The relatively fast saturation of ice Ih is due to the small pore sizes; at saturation, where three H<sub>2</sub> molecules are stored in each fundamental unit cell (12 molecules), occupying 55% of the available volume.

We calculate the H<sub>2</sub>–ice Ih binding energy to be  $12.8 \pm 0.02$  kJ/mol at 77 K and 40 bar, significantly larger than the 3–4 kJ/mol of materials relying on physisorption with weak vdW interactions.<sup>22</sup> The quadrupole (H<sub>2</sub>)–dipole (H<sub>2</sub>O) interaction helps stabilize the H<sub>2</sub>–ice structures, accounting for all of the binding, with the vdW forces always repulsive to act as a counter-balance to the favorable electrostatic forces. This calculated binding energy is about half the value 22–25 kJ/mol suggested for optimal storage near room temperature,<sup>23</sup> which explains the reduction in the storage capacity at 100 bar and 150 K (4.1 wt %), 175 K (3.1 wt %), 200 K (1.98%). At the ice melting temperature of 270 K and 100 bar, we calculate 0.4 wt % H<sub>2</sub> uptake by ice Ih, 3 times the capacity of carbon nanotubes and porous carbon

materials, but comparable to the 1.0 wt % for MOF-177 and 1.25% for MOF-200.<sup>21</sup>

Figure 1c shows the volumetric uptake (density) of H<sub>2</sub> stored in ice Ih, amorphous ice, and in a hydrogen tank. At a constant pressure of 50 bar and 77 K, we find that ice Ih stores twice the amount of hydrogen as the hydrogen tank, while at 100 K ice stores 3 times as much and at 150 K, 4 times as much. Beyond 150 K, the relative storage capacity of H<sub>2</sub> in ice Ih is significantly reduced as the thermal energy of the system overcomes the H<sub>2</sub>–H<sub>2</sub>O binding energy. Of note is that below 150 K and every pressure considered here, ice Ih stores 3–5 times more H<sub>2</sub> than amorphous ice, illustrating the uniqueness of the hexagonal channels for H<sub>2</sub> storage.

To investigate the process of loading, we carried out MD simulations of a 1 nm thick ice Ih slab ( $0.35 \times 0.38$  nm<sup>2</sup> surface area) exposed to H<sub>2</sub> gas (Figure 2a). Here ice Ih was loaded with H<sub>2</sub> obtained from GCMC calculations at 100 bar and 150 K, using an outside gas pressure of 150 bar. This system achieved thermal and mass balance after 23 ns, storing 3.98 wt % H<sub>2</sub> (which leads to an internal gas pressure of  $130 \pm 25$  bar). The 3.98 wt % at 100 bar and 150 K from our MD simulations agrees with the 4.07 wt % we calculate using GCMC. Under these conditions, we observe a sustained exchange rate of 2 H<sub>2</sub> molecules/ns in and out of the ice surface (Figure 2b), which decreases to 1.7 molecules/ns after 62 ns due to distortion of the surface layers obstructing exit from the hexagonal channels. This surface disorder extends two layers into the crystal (Figure 2d). Similar simulations at 100 K and 40 bar (the saturation pressure) show little distortion of the ice Ih surface on the same time scale, most likely due to the lower energy of the H<sub>2</sub> molecules. Since the surface atoms of ice Ih have 1 fewer hydrogen bonds than the bulk, they would “melt” at a lower temperature, leading to a “Tammann temperature” for ice Ih of 180 to 200 K.<sup>24–26</sup> The disordered layer we observe in the MD at 150 K likely results from collisions with the high pressure (150 bar) external gas, but it may also reflect a limitation of the TIP4P-ice water model, which was not parametrized to describe free surfaces. Thus, the lack of polarization in this model may destabilize the surface layer, leading to a decreased Tammann temperature. This MD treats the vibrational energy states of water and H<sub>2</sub> as classical, whereas they should be in the lowest quantized vibrational level. We expect this to lead to negligible error in the loading curves.

To investigate the effect of a disordered surface layer on the H<sub>2</sub> storage ability of ice Ih, we equilibrated the 4.07 wt % GCMC structure, capped with a 0.5 nm thick amorphous ice layer. We

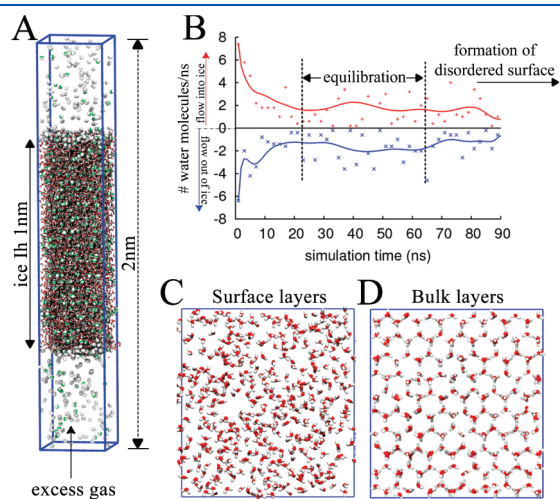


**Figure 2.** (A) Schematic of simulation cell used for MD simulations of the loading process. A 1 nm deep ice Ih slab is first loaded with H<sub>2</sub> at 100 bar and 150 K using our GCMC procedure. It is then immersed in a pre-equilibrated box of H<sub>2</sub> molecules at 150 bar, removing any overlapping H<sub>2</sub> molecules. (B) The flow rate of H<sub>2</sub> molecules into the ice structure (red crosses) and out of the ice (blue stars) as a function of time. The solid lines are best fits based on the cubic Bezier function approximations. There is a net flow of H<sub>2</sub> molecules into the ice until 23 ns when the system reaches thermodynamic equilibrium. After 62 ns, the surface layers start becoming disordered due to molecular vibrations and collisions with the outside H<sub>2</sub> molecules. (C) Snapshot of the ice surface after 90 ns of simulation, showing the formation of an amorphous layer  $\sim 0.8$  nm thick. (D) Comparative snapshot of the middle ice layer, showing that the integrity of the hexagonal framework is maintained.

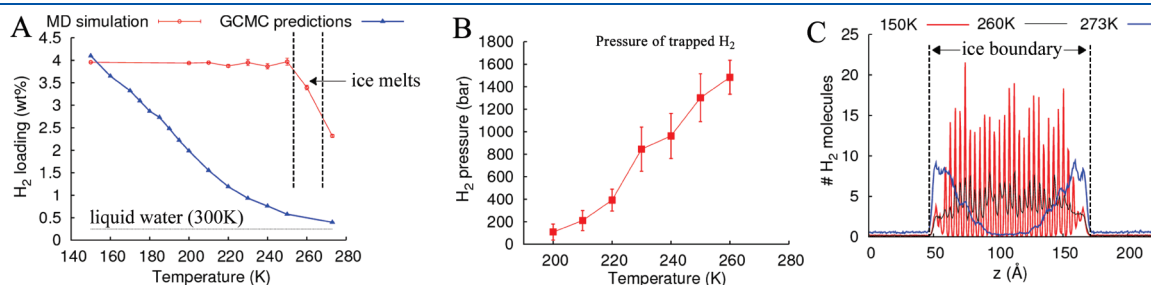


**Figure 3.** (A) Comparison of H<sub>2</sub> uptake as a function of temperature. The initial MD system consists of the GCMC optimized structure at 150 K and 100 bar (4.07 wt % H<sub>2</sub>) with a 0.2 nm amorphous ice layer capping each end surrounded by a vacuum. The structure is stable up to 265–270 K, when the ice melts abruptly. (B) The pressure that the trapped H<sub>2</sub> gas exerts on the ice framework. Before melting, the H<sub>2</sub> exerts 1562 bar of pressure on the ice. (C) Average H<sub>2</sub> density along the direction normal to the capped ice surface at 150 K (red line), 260 K (black line), and 273 K (blue line). The ice extends from 5 to 15 nm on the *x* axis. The H<sub>2</sub> did not completely diffuse out of the water slab on the 50 ns time scale of our simulations; however, the shape and nonuniformity of the distribution indicates a gradual process of segregation.



find the capped nanocube is stable on our entire simulation time scale (90 ns) at 150 K, with no exchange of H<sub>2</sub> out of the ice. Indeed, the system is thermodynamically stable up to 265 K (Figure 3a), even though the internal H<sub>2</sub> pressure rises to 1582 ± 204 bar by 265 K (Figure 3b). Between 265 and 270 K, the ice melts, causing 93.9% of the stored H<sub>2</sub> to evolve from the ice (because of the low solubility of H<sub>2</sub> in liquid water).

These results lead us to propose the ice-fixed melt-triggered (IFMT) strategy for hydrogen storage and utilization with ice as the median:

- load the H<sub>2</sub> at 100 K and 40 bar in crystalline ice Ih,
- seal the surfaces at 150 K and 250 bar external H<sub>2</sub> pressure,
- store between 150 and 265 K in low pressure gas until needed, and
- trigger evolution of the stored H<sub>2</sub> by changing the temperature slightly to just above melting, releasing 94% of the stored H<sub>2</sub>.

On the time scale of our simulations, our results indicate that neglecting any contributions due to the small capping layer, this process would lead to  $4.07 \times 0.94 = 3.8$  wt % usable H<sub>2</sub> storage and 42 g L<sup>-1</sup> at 265 K, within range of the US DOE 2010 requirements for transportation: 6.0 wt % and 45 g L<sup>-1</sup> at 243–358 K.<sup>3</sup> Of course there are many practical problems of forming high surface area crystals of ice quickly, sealing the surface, and then storing the system after loading the H<sub>2</sub>, maybe in dry ice. However the enormous advantages of extremely low cost and wide availability of the storage material and the greenness in producing, using and disposing of the storage provides significant advantages that make the IFMT strategy worthy of additional study. Moreover, the IFMT mechanism presents a new paradigm for hydrogen storage that might produce even more efficient hydrogen storage materials.

## ■ ASSOCIATED CONTENT

Supporting Information. Computational methods, Table S1, Figures S1–S5 and references. This material is available free of charge via the Internet at <http://pubs.acs.org>.

## ■ ACKNOWLEDGMENT

The authors thank Jose Mendoza (Caltech) and Sang Soo Han (KRISS, Korea) for providing data on H<sub>2</sub> storage in MOFs prior to publication. This project was partially supported by grants to Caltech from the Department of Energy (DE-PS36-08GO 98004P). It was also supported by the WCU program (31-2008-000-10055-0) through the National Research Foundation of Korea with the generous allocation of computing time from the KISTI supercomputing center. T.A.P. thanks the U.S. Department of Energy CSGF and the National Science Foundation for graduate fellowships.

## ■ REFERENCES

- (1) Abascal, J.; Sanz, E.; Fernandez, R.; Vega, C. A Potential Model for the Study of Ices and Amorphous Water: Tip4p/Ice. *J. Chem. Phys.* **2005**, *122*, 234511.
- (2) Schlapbach, L.; Züttel, A. Hydrogen-Storage Materials for Mobile Applications. *Nature* **2001**, *414*, 353–358.
- (3) Satyapal, S.; Petrovic, J.; Read, C.; Thomas, G.; Ordaz, G. The U.S. Department of Energy's National Hydrogen Storage Project: Progress Towards Meeting Hydrogen-Powered Vehicle Requirements. *Catal. Today* **2007**, *120*, 246–256.

- (4) Wong-Foy, A. G.; Matzger, A. J.; Yaghi, O. M. Exceptional H<sub>2</sub> Saturation Uptake in Microporous Metal–Organic Frameworks. *J. Am. Chem. Soc.* **2006**, *128*, 3494–3495.

- (5) Strauss, H. L.; Chen, Z.; Loong, C. K. The Diffusion of H<sub>2</sub> in Hexagonal Ice at Low Temperatures. *J. Chem. Phys.* **1994**, *101*, 7177–7180.

- (6) van der Waals, J. H.; Platteeuw, J. C. *Clathrate Solutions*; John Wiley & Sons, Inc.: New York, 1959.

- (7) Franks, F. *Water. A Comprehensive Treatise. 2. Water in Crystalline Hydrates, Aqueous Solutions of Simple Nonelectrolytes*; Plenum Press: New-York/London, 1973.

- (8) Landolt, B.; Schäfer, K.; Lax, E. *Zahlenwerte und Funktionen aus Physik, Chemie, Astronomie, Geophysik und Technik. Band 2, Teil 2, Bandteil B, Eigenschaften der Materie in Ihren Aggregatzuständen. Gleichgewichte Ausser Schmelzgleichgewichten. Lösungsgleichgewichte I*; Springer: Berlin, 1962.

- (9) Mao, W. L.; Mao, H. K.; Goncharov, A. F.; Struzhkin, V. V.; Guo, Q. Z.; Hu, J. Z.; Shu, J. F.; Hemley, R. J.; Somayazulu, M.; Zhao, Y. S. Hydrogen Clusters in Clathrate Hydrate. *Science* **2002**, *297*, 2247–2249.

- (10) Mao, W. L.; Mao, H. K. Hydrogen Storage in Molecular Compounds. *Proc. Natl. Acad. Sci. U. S. A.* **2004**, *101*, 708–710.

- (11) Lee, H.; Lee, J.-w.; Kim, D. Y.; Park, J.; Seo, Y.-T.; Zeng, H.; Moudrakovski, I. L.; Ratcliffe, C. I.; Ripmeester, J. A. Tuning Clathrate Hydrates for Hydrogen Storage. *Nature* **2005**, *434*, 743–746.

- (12) Dyadin, Y. A.; Aladko, E. Y.; Udachin, K. A.; Tkacz, M. The Solubility of Helium and Hydrogen in Ice Ih at High-Pressures. *Polym. J. Chem.* **1994**, *68*, 343–348.

- (13) Londono, D.; Kuhs, W. F.; Finney, J. L. Enclathration of Helium in Ice-II - The 1st Helium Hydrate. *Nature* **1988**, *332*, 141–142.

- (14) Phillips, T. R.; Maluendes, S.; Mclean, A. D.; Green, S. Anisotropic Rigid Rotor Potential-Energy Function for H<sub>2</sub>O–H<sub>2</sub>. *J. Chem. Phys.* **1994**, *101*, 5824–5830.

- (15) Patkowski, K.; Cencek, W.; Jankowski, P.; Szalewicz, K.; Mehl, J. B.; Garberoglio, G.; Harvey, A. H. Potential Energy Surface for Interactions between Two Hydrogen Molecules. *J. Chem. Phys.* **2008**, *129*, 094304.

- (16) Leachman, J. W.; Jacobsen, R. T.; Penoncello, S. G.; Lemmon, E. W. Fundamental Equations of State for Parahydrogen, Normal Hydrogen, and Orthohydrogen. *J. Phys. Chem. Ref. Data* **2009**, *38*, 721–748.

- (17) The GCMC simulations reported here used the sorption module of Cerius2 (Accelrys, San Diego) with our ab initio FF. The results reported herein are for excess H<sub>2</sub> uptake as in ref 20.

- (18) Garberoglio, G.; Skoulidas, A. I.; Johnson, J. K. Adsorption of Gases in Metal Organic Materials: Comparison of Simulations and Experiments. *J. Phys. Chem. B* **2005**, *109*, 13094–13103.

- (19) Barnes, W. H. The Crystal Structure of Ice between 0 °C and –183 °C. *Proc. R. Soc. London, Ser. A* **1929**, *125*, 670–693.

- (20) Bernal, J. D.; Fowler, R. H. A Theory of Water and Ionic Solution, with Particular Reference to Hydrogen and Hydroxyl Ions. *J. Chem. Phys.* **1933**, *1*, 515–548.

- (21) Han, S. S.; Deng, W. Q.; Goddard, W. A. Improved Designs of Metal–Organic Frameworks for Hydrogen Storage. *Angew. Chem., Int. Ed.* **2007**, *46*, 6289–6292.

- (22) Murray, L. J.; Dinca, M.; Long, J. R. Hydrogen Storage in Metal–Organic Frameworks. *Chem. Soc. Rev.* **2009**, *38*, 1294–1314.

- (23) Garrone, E.; Bonelli, B.; Otero Areán, C. Enthalpy–Entropy Correlation for Hydrogen Adsorption on Zeolites. *Chem. Phys. Lett.* **2008**, *456*, 68–70.

- (24) Golecki, I.; Jaccard, C. Intrinsic Surface Disorder in Ice near the Melting Point. *J. Phys. C: Solid State Phys.* **1978**, *11*, 4229.

- (25) Suter, M. T.; Andersson, P. U.; Pettersson, J. B. C. Surface Properties of Water Ice at 150–191 K Studied by Elastic Helium Scattering. *J. Chem. Phys.* **2006**, *125*, 174704–174706.

- (26) Wei, X.; Miranda, P. B.; Zhang, C.; Shen, Y. R. Sum-Frequency Spectroscopic Studies of Ice Interfaces. *Phys. Rev. B* **2002**, *66*, 085401.